ELSEVIER

Thermochimica Acta 313 (1998) 27–36

thermochimica acta

Precipitation kinetics in an air-cooled aluminum alloy: A comparison of scanning and isothermal calorimetry measurement methods

George W. Smith*

Department of Physics and Physical Chemistry, General Motors Research and Development Center, Warren MI, 48090-9055, USA

Received 23 May 1997; received in revised form 30 October 1997; accepted 12 November 1997

Abstract

The purpose of this work is to establish for the first time the equivalence of determinations of both precipitation time constants, τ, and activation energies, E_{act}, by two calorimetric techniques: differential scanning calorimetry (DSC) and differential isothermal calorimetry (DIC). To accomplish this, kinetics and energetics of precipitation in air-cooled (ACO) aluminum alloy 339 were determined by both methods, using Perkin–Elmer instruments. The ACO alloy was chosen as the subject of the study because of its calorimetric simplicity: a single precipitation exotherm dominates each DSC scan. The DSC data were analyzed using a modified Kissinger equation, from which both time constants and activation energies were derived. From differential isothermal calorimetry experiments, we determined precipitation time constants by fitting the almost exponential decay of DIC heat release curves, using analyses developed in our laboratory. Arrhenius plots of the time constants then yielded values of E_{act}. Both activation energies and time constants from the DSC/Kissinger analysis agreed rather well with those from DIC provided DSC temperature scan rates were slow compared to the calorimeter's instrumental equilibration time (lag time). Thus, the equivalence of the DSC and DIC techniques has been established, at least for this test case. © 1998 Elsevier Science B.V.

Keywords: Aluminum alloy; Differential isothermal calorimetry; Differential scanning calorimetry; Kissinger analysis; Precipitation kinetics

1. Introduction

Precipitation in aluminum alloys has been studied by many investigators [1–23] using differential scanning calorimetry (DSC). Several analytical schemes [24–28] have been advanced to determine kinetic parameters (e.g. time constants, τ, and activation energies, E_{act}) from the scan-rate dependence of peaks observed in DSC curves. Two review articles examine these and related analysis methods in detail [29,30].

As yet there appears to be no publication which comprehensively compares DSC kinetics parameters to those derivable from differential isothermal calorimetry (DIC), a technique [19,31–38] which has not been widely applied to precipitation studies but which has certain advantages relative to DSC. The most

*Corresponding author. Tel.: 00 1 810 986 0614; fax: 00 1 810 986 3091; e-mail: gsmith@cmsa.gmr.com

PII S0040-6031(97)00452-8

extensive isothermal calorimetry precipitation studies to date seem to have been carried out using a Tian–Calvet microcalorimeter (TCM), a device whose sensitivity limits its application to processes which start slowly (>30 min) [39–46]. In contrast, DIC (using a Perkin–Elmer DSC2 instrument) can be applied to systems with time constants of the order of minutes. While there have been numerous DSC investigations, apparently no DIC determinations of τ or E_{act} values for precipitation in alloys have been reported. And, of course, there also has been no direct comparison of the two methods. Lacom et al. [45] have determined the activation energy for GP zone formation in an Al/Zn alloy using both isothermal Tian–Calvet calorimetry and DSC in a cooling mode, obtaining comparable values of E_{act} with an error of $\pm 10\%$ (somewhat larger, as will be seen below, than the 5 to 6% error attained from DIC and DSC). Starink and Zahra [46] have determined E_{act} for precipitation in an Al/Mg alloy using isothermal TCM.

It is the purpose of this work to establish for the first time the equivalence of DSC and DIC measurements of precipitation τ and E_{act} values. To accomplish this, kinetics and energetics of precipitation in air-cooled (ACO) aluminum alloy 339 were determined by both methods. The ACO alloy was chosen as the subject of the study because of its calorimetric simplicity: only a single precipitation exotherm is observed in a DSC scan. Values of τ and E_{act} were obtained from our DSC scans using a modified Kissinger equation [24,28] which relates the peak precipitation temperature, T_p, to the temperature scan rate, S, of the calorimeter. From our DIC experiments, we determined precipitation time constants using several analysis methods developed in our laboratory. Arrhenius plots of the temperature-dependent time constants then yielded activation energies. In addition, accurate values of ΔQ, the heat released during the precipitation process, were obtained from DIC.

In the next sections, we shall compare the results derived from the Kissinger/DSC analysis with those from DIC and show that they agree rather well, provided the DSC temperature scan rate is slow compared to the calorimeter's instrumental lag time, τ_{lag}. Thus, the equivalence of the two methods will be established for this alloy.

First, let us briefly discuss the experimental details of the work.

2. Experimental aspects

2.1. Samples

Aluminum alloy 339 contains ~1% Cu, ~1% Mg and ~12% Si (by mass), plus smaller amounts of other species. Calorimetry samples were cut from a casting which had been air-cooled (ACO) immediately after solidification; the samples were then stored at room temperature for ca. 17 months, after which the calorimetric studies were carried out. In the die the casting had cooled to ~300°C in a few seconds; after removal from the die, its cooling rate in air was so slow (6–10 h to reach ambient) that GP zones could form and then mostly re-dissolve before ambient temperature was reached. Consequently, no GP zone formation exotherms were detected in DSC scans, although there is slight evidence for a possible GP zone dissolution endotherm just below the single precipitation exothermic peak in the scans of Fig. 1. The fact that the DSC scans are calorimetrically simple facilitated the comparison of the DSC and DIC methods (as will be seen below). Preliminary calorimetry experiments showed that the alloy was quite stable at room temperature: the

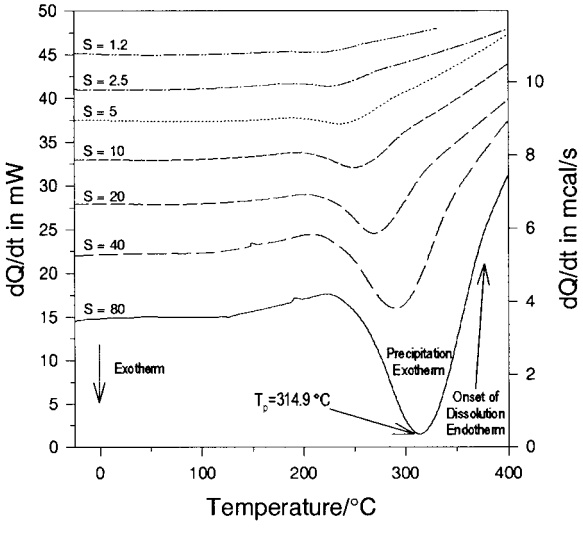

Fig. 1. Plots of dQ/dt vs. temperature for air-cooled alloy 339 run at scan rates from 1.2 to 80°C min^{-1}. The exothermic peak for each curve is due to precipitation in the alloy. The peak temperature, T_p, is shown for the 80°C min^{-1} curve. The values of T_p are used in Eqs. (1) and (3) to derive effective activation energies. The curves are shifted vertically to avoid overlap.

DSC signal changed very little over periods as long as two years.

Samples of the proper size for calorimetry were prepared in the following manner: Rods of square cross section were cut from the casting and machined to cylinders with a diameter of 6 mm. Thin slices (~2 mm thick) were then cut from these rods. Sample masses, m, ranged 115–137 mg.

2.2. Calorimetric methods

The kinetics and energetics of precipitation were determined using Perkin–Elmer DSC2 and DSC7 differential scanning calorimeters, operation of which has been described previously [31–38]. In the present work, the DSC7 instrument was used in its temperature-scanning mode and the DSC2 in its isothermal mode. As a scanning instrument, the calorimeter gives a broad view of the temperature range and amount of heat released (ΔQ) during the precipitation. More detailed information regarding the rate of heat release and more accurate ΔQ values are obtained from isothermal measurements as a function of temperature. In the next sections, we briefly examine the scanning and isothermal calorimetry techniques.

2.2.1. Differential scanning calorimetry (DSC)

In the DSC mode the calorimeter measures dQ/dt, the rate of heat absorption or emission by the sample, as a function of temperature. In the absence of any significant thermal events, the position of the baseline in such a plot is proportional to the specific heat of the sample [34,37,38]. The presence of an endothermic peak, superimposed on the baseline, indicates the occurrence of a heat-absorbing event, such as melting or species dissolution. On the other hand, an exothermic peak occurs as a result of some sort of heat-releasing event, such as solidification or precipitation. The area under a peak is proportional to ΔQ, the heat absorbed or released by the sample over the temperature range of the peak. However, the ΔQ values obtained for a precipitation exotherm are only approximate because of the onset of an endotherm (due to dissolution of precipitates) at temperatures just above the exotherm (e.g. see Fig. 1). ΔQ values (8–10 J/g) obtained from DSC scans of Fig. 1 are consistent with the more accurate results obtained by DIC (see Section 3.2.2).

2.2.2. Differential isothermal calorimetry (DIC)

Operated isothermally, the calorimeter records dQ/dt vs. time at a specific temperature. A typical DIC curve for precipitation in ACO alloy 339 at 220°C is shown in Fig. 2. In such an experiment, the sample temperature is increased very rapidly (320°C min^{-1}) from −73°C to the desired temperature, T. For a short time after T is reached, the data are invalid (off-scale) due to non-equilibrium conditions. This interval roughly defines the instrumental lag time, τ_{lag}, which can be determined by measuring the time required for the calorimeter signal to return to its normal range. (As seen in Fig. 2, this time interval – even for samples as heavy as 100 mg – is quite short, ~1 min). Although the missing data for times shorter than τ_{lag} can be taken into account by analytic techniques [31], for our ACO alloy the data loss is minimal because τ_{lag} is so short.

Another concern in analyzing DIC curves is baseline drift, which can result from thermal imbalances between the sample and reference pans of the calorimeter, leading to modest, more or less linear, changes in baseline position during the course of an experiment. Generally, drift is significant only for very weak

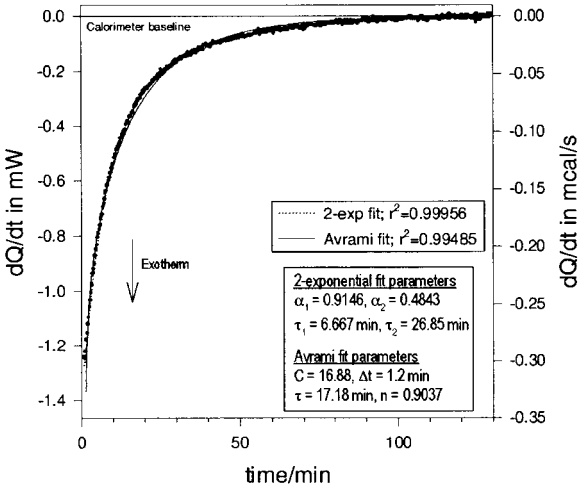

Fig. 2. Isothermal calorimetry curve of dQ/dt vs. time for precipitation in a sample of air-cooled alloy 339 at 220°C. The time at which the final temperature is reached after the initial rapid warm-up is taken to be t=0. Although the duration of the experiment was 280 min, precipitation was essentially complete within the first 2 h. Only the first 130 min of data are shown in order to make clear the fits of analytical expressions (see text), which yielded values of the precipitation time constant(s).

exotherms and/or experiments of extremely long duration (many hours). Methods to correct the DIC signal for baseline drift have been described elsewhere [32]. In most cases, such corrections are small since by thoroughly isolating the calorimeter head and using pure aluminum references with masses comparable to those of the samples, we have reduced sources of calorimeter imbalance.

As for DSC scans, isothermal dQ/dt curves can be either endothermic or exothermic, depending on the nature of the thermal process involved. Accurate values of the total energy, ΔQ, absorbed or released during an isothermal process, are determined by integrating dQ/dt vs. t.

3. Analysis methods

It is appropriate at this time to examine in some detail the analytical methods used to determine precipitation kinetics from both DSC and DIC.

3.1. Scanning experiments: Kissinger analysis

The Kissinger method [24,28] for deriving activation energies from temperature-scanned experiments is based on the fact that the observed temperature of a peak depends on the scan rate, $S=dT/dt$, of the experiment. The method has been generalized and justified for solid-state reactions by Mittemeijer et al. [28]. Peaks for slow scan rates occur at lower temperatures than those for fast scan rates. This shift of peak temperature, T_p, with a change in scan rate is clearly seen in Fig. 1, where dQ/dt is plotted versus temperature for precipitation in ACO alloy 339 at scan rates ranging 1.2–80°C min^{-1}. (We shall see below that it is important to use the slower scan rates, eliminating data for S=40 and 80°C min^{-1}.) As is well known, the peak intensity greatly decreases as scan rate is reduced. In Fig. 1, we see the onset of the previously mentioned high temperature dissolution endotherm which, although it interferes with evaluation of ΔQ, does not greatly affect the determination of the peak temperature. The Kissinger expression, as modified by Mittemeijer et al. [28], relates T_p to S:

$$\ln(T_p^2/S) = E_{act}/(RT_p) + \ln(E_{act}/Rk_0). \quad (1)$$

Here, E_{act} is the effective activation energy for the process associated with the peak, R the gas constant, and k_0 the pre-exponential factor in the Arrhenius equation for the rate constant k:

$$k = k_0 \exp(-E_{act}/RT) \quad [\text{or } \tau \equiv 1/k = \tau_0 \exp(E_{act}/RT)]. \quad (2)$$

It is easy to show that substitution of Eq. (2) into Eq. (1) yields a simple expression for k_p, the value of k at temperature T_p:

$$k_p = (E_{act}/R) \times (S/T_p^2), \quad (3)$$

In Eqs. (1) and (3), S is given in K s^{-1} (or °C s^{-1}) so that k has units of s^{-1}. Values of S and T_p corresponding to the curves of Fig. 1 are given in Table 1.

The extent to which the Kissinger method is valid has been discussed by Yinnon and Uhlmann [29] who

Table 1
Parameters for Kissinger fits to scanning experiments. Air-cooled aluminum alloy 339. Kissinger rate constant (from Eq. (2)) k_0=1.405(+3.90/−1.03)×10^8 s^{-1}

ID	S (°C min^{-1})	T_p (°C)	$1000/RT_p$	$\ln(T_p^2/S)$	Fit of Eq. (1) for S<40°C min^{-1}
HC10A	1.2	217.68	1.02524	16.3044	16.1071
HC9A	2.5	227.00	1.00614	15.6081	15.6332
EF3A	5	237.25	0.98594	14.9555	15.1319
EF4A	10	252.12	0.95803	14.3198	14.4395
EE13A	20	270.79	0.92515	13.6965	13.6238
EF1A	40	293.05	0.88878	13.0835	
EF2A	80	314.91	0.85574	12.4661	

Note: In carrying out the Kissinger analysis, it is necessary to use S values in units of °C/s.
See text for discussion of regression fits shown in column six.

reviewed seven methods for analyzing scanning thermoanalytical data. They were concerned that the original Kissinger method might not be generally applicable to solid-state transformations. However, Mittemeijer et al. [28] examined the Kissinger analysis in detail and concluded that activation energies can indeed be obtained from Eqs. (1) and (2), but that appreciable error in k_0 can occur if Eq. (2) is extrapolated to $1/T=0$. Nevertheless, we have found (see Section 4.2.2) that for sufficiently slow scan rates, it is still possible to obtain values of $1/k$ (the reciprocal of the Kissinger rate constant) which agree with isothermal precipitation time constants in the experimental temperature range.

The Kissinger method is validated in Fig. 3 where we plot two linear regression fits of Eq. (1), using values of T_p derived for alloy 339 from DSC curves like those of Fig. 1. One fit includes data for all scan rates, the other eliminates results for $S=40$ and $80^\circ C\ min^{-1}$. By excluding the data for these high scan rates, we reduce the effects of τ_{lag}. The exclusion of these data is justified in Section 4.1, where we develop a criterion for choosing valid S values and comparing E_{act} values from scanning methods with those from analyses of isothermal curves.

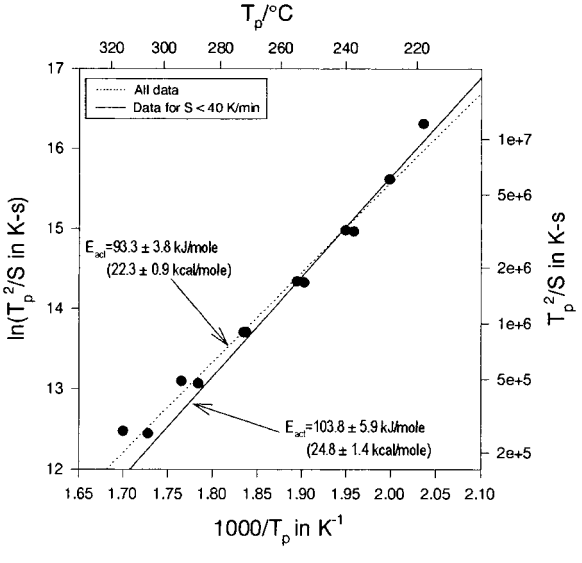

Fig. 3. Kissinger plot for air-cooled alloy 339. The lines are fits of Eq. (1) to the data, as discussed in the text. T_p is quite sensitive to scan rate, ranging from ca. 220°C for $S=1.2^\circ C\ min^{-1}$ to ca. 315°C for $S=80^\circ C\ min^{-1}$.

3.2. Isothermal experiments

We shall illustrate our DIC analyses using the curve of Fig. 2. As will become apparent, the same precipitation process is responsible for the DSC peaks of Fig. 1 and isotherms like that of Fig. 2. From such isotherms it is possible to derive time constants by fitting analytical expressions to the decay of dQ/dt with time. Arrhenius plots of time constants determined from isothermal experiments at various temperatures yield precipitation activation energies. Some of the analyses and resulting time constants have been discussed elsewhere [31,32], so the following description is brief.

3.2.1. Time constants

3.2.1.1. 2-Exponential analysis. This analysis can be justified by assuming that two species precipitate simultaneously, so that the rate of heat evolution at a given temperature is given by:

$$dQ/dt = -\alpha_1 \exp(-t/\tau_1) - \alpha_2 \exp(-t/\tau_2), \tag{4}$$

where each of the exponential terms represents the precipitation kinetics of a single species. Although TEM studies [47] have indicated that two or more precipitate phases are indeed involved, a strictly mathematical interpretation of Eq. (4) is also possible, i.e. it is merely the first two terms in a series approximation to the data. In Fig. 2, the 2-exponential expression essentially coincides with the data. The temperature dependences of the fast (τ_1) and slow (τ_2) processes are usually well described by the Arrhenius equation as seen in Fig. 4. Values of α and τ, corresponding to the data of Fig. 4, are given in Table 2.

3.2.1.2. Rate-averaged τ from 2-exponential analysis. For simultaneous processes which contribute to the same precipitation event the physically meaningful time constant [48] is the rate-averaged time constant, τ_{rate}. Such an average time constant is useful for comparison of isothermal results with those from scanning calorimetry, and is defined in terms of the 2-exponential fit parameters:

$$1/\tau_{rate} = (\alpha_1/\tau_1 + \alpha_2/\tau_2)/(\alpha_1 + \alpha_2). \tag{5a}$$

$$\tau_{rate} = \tau_1\tau_2(\alpha_1 + \alpha_2)/(\alpha_1\tau_2 + \alpha_2\tau_1). \tag{5b}$$

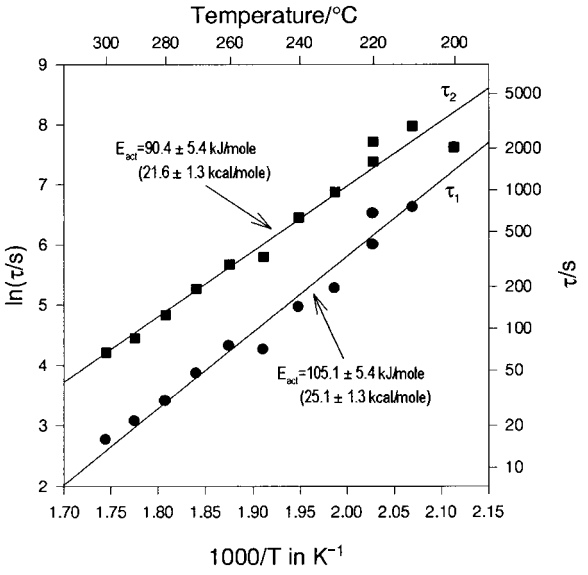

Fig. 4. Arrhenius plots of τ_1 and τ_2 derived from 2-exponential fits to isothermal dQ/dt curves for air-cooled alloy 339. Generally, the coefficient α_1 for the short time constant τ_1 is appreciably greater than α_2, the coefficient for τ_2, the long time constant. Lines are best fits to the data.

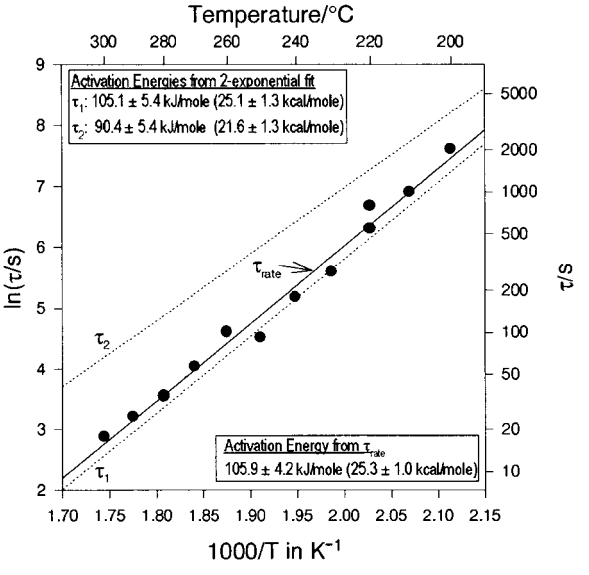

Fig. 5. Comparison of Arrhenius plot of τ_{rate} derived from the data of Fig. 4 and Table 2 (• and ———) with regressions of 2-exponential time constants, τ_1 and τ_2, from Fig. 4 (· · ·). It seems that τ_{rate} is dominated by the fast precipitation process, τ_1.

In Fig. 5, an Arrhenius plot of τ_{rate} for the α and τ values of Table 2 is compared with the regression fits for τ_1 and τ_2 of Fig. 4. The value of E_{act} for τ_{rate} is practically equal to that for τ_1. Furthermore, τ_{rate} is only slightly larger than τ_1, so that it seems clear that the fast process dominates precipitation in air-cooled alloy 339.

3.2.1.3. Avrami analysis. As discussed elsewhere [31,32], the kinetics of phase transformations,

Table 2
2-exponential and Avrami analyses of isothermal experiments. Air-cooled aluminum alloy 339

2-exponential analysis									Avrami analysis			
ID	T (°C)	$-\Delta Q$ (J/g)	α_1 (mW)	α_2 (mW)	τ_1 (min)	τ_2 (min)	r^2	τ_{rate} (min)	Δt (min)	τ (min)	n	r^2
EH2A	200	4.96	0.0761	0.2429	33.84	33.850	0.98625	33.85	4.50	32.33	1.0392	0.98881
EH9A	210	9.50	0.5291	0.2771	12.37	48.350	0.99336	16.62	2.60	30.53	0.917	0.98804
EG4A	220	9.15	0.8837	0.2491	11.2	37.268	0.99913	13.23	1.001	8.34	0.936	0.99498
EH11A	220	9.28	0.9146	0.4843	6.667	26.850	0.99956	9.01	1.201	7.18	0.904	0.99485
EG3A	230	9.03	1.5584	0.8238	3.229	15.970	0.99922	4.46	0.751	0.97	0.861	0.99532
EH6A	240	9.67	3.5560	1.2118	2.358	10.574	0.99982	2.94	0.60	5.747	0.89	0.99160
EG6A	250	9.35	5.9659	2.4685	1.186	5.463	0.99970	1.54	0.50	3.587	0.857	0.99606
EH7A	260	9.30	5.6624	3.0106	1.244	4.834	0.99989	1.68	0.60	3.27	0.929	0.99439
EH1A	270	9.54	13.366	3.4844	0.792	3.226	0.99985	0.94	0.40	1.737	0.87	0.99491
EH8A	280	8.54	26.263	5.9990	0.5	2.085	0.99975	0.58	0.50	1.197	0.915	0.99268
EH4A	290	7.64	35.715	7.8701	0.359	1.422	0.99978	0.41	0.35	0.833	0.869	0.99588
EH10A	300	8.35	55.155	9.3641	0.264	1.121	0.99970	0.30	0.30	0.612	0.884	0.99405

including precipitation, are frequently well described by the Avrami equation:

$$X(t) = 1 - \exp[-(t/\tau_{\text{Avrami}})^n], \quad (6)$$

where $X(t)$ is the fraction of material transformed or precipitated, t the time, τ_{Avrami} is an average time constant, and n is a constant. The values of τ_{Avrami} can be derived from isothermal data by fitting the decaying portion of the dQ/dt curves to the equation [32]:

$$dQ/dt = -C \times \exp(-((t - \Delta t)/\tau_{\text{Avrami}})^n) \times (n(t - \Delta t)^{n-1}/\tau^n_{\text{Avrami}}), \quad (7)$$

where C is a constant and Δt is a time shift of the order or larger than τ_{lag} or the time for the extremum value of dQ/dt [49]. This equation is quickly and accurately fit directly to experimental dQ/dt curves by means of appropriate software, such as TableCurve [50], to yield the Avrami parameters shown in Table 2. In Fig. 2, in addition to the 2-exponential fit, we show a best fit of Eq. (7) to dQ/dt. It is clear that the fit of the Avrami expression, while good, does not represent the data as well as the 2-exponential equation. An Arrhenius plot of Avrami time constants for the ACO alloy is shown in Fig. 6. The derived activation energy is somewhat smaller than the value from τ_{rate} and τ_1.

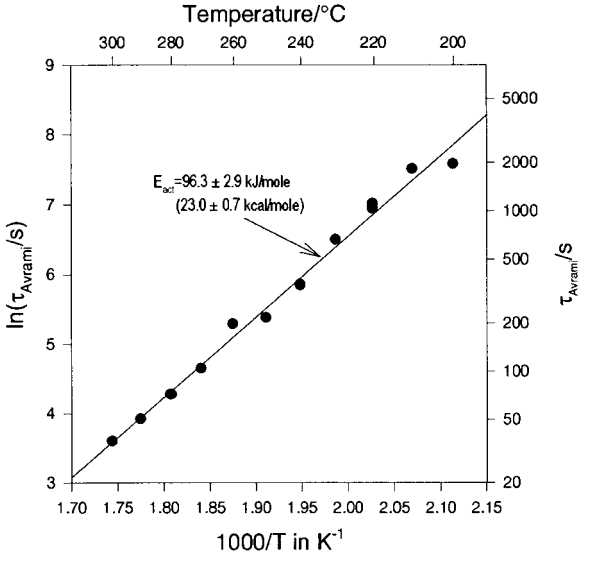

Fig. 6. Arrhenius plot of τ_{Avrami} for air-cooled alloy 339. The line is a best fit to the data.

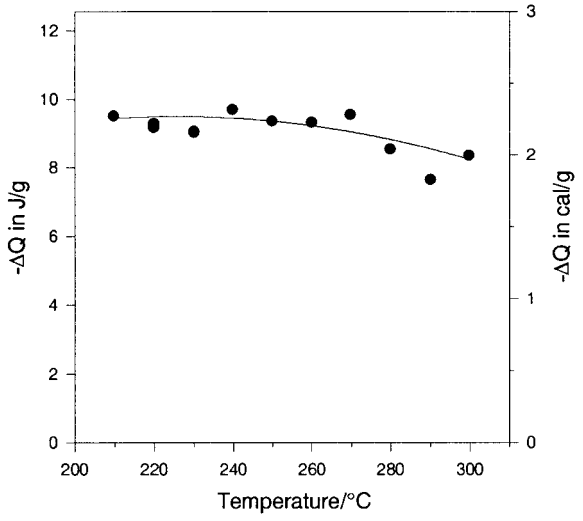

Fig. 7. Heat released, ΔQ, during precipitation in air-cooled alloy 339 at various temperatures. ΔQ values were determined from isothermal calorimetry curves of dQ/dt vs. time like that of Fig. 2.

3.2.2. ΔQ, the total heat release from isothermal experiments

As already mentioned, ΔQ, the heat released during the precipitation, is determined by integrating dQ/dt; thus, the curve of Fig. 2 yields $\Delta Q = -9.28$ J/g. Fig. 7 plots $-\Delta Q$ vs. T for the air-cooled alloy 339. The slight decrease in values of $-\Delta Q$ at high temperatures is probably due to loss of early time data as the precipitation time constant becomes comparable to τ_{lag}. The value at 200°C in Table 2 is anomalously low due to signal-to-noise considerations and has been excluded from the plot.

4. Results and discussion

4.1. Scanning calorimetry

Parameters and a regression fit for the Kissinger analysis of the DSC results for ACO alloy 339 are given in Table 1. Columns one to three give the DSC sample identification, scan rate, and peak temperature. The next two columns list the dependent and independent variables for the Kissinger equation. The sixth column gives the results of a linear regression fit to Eq. (1) for S<40°C min^{-1}. Also

given in the table is the k_0 value and its error from Eq. (2). As predicted by Mittemeijer et al. [28] the error in k_0 is appreciable.

To obtain the best values of activation energy from the Kissinger analysis, it is important to account for τ_{lag}, the equilibration time of the calorimeter, which can result in a time 'lag' between the recorded and 'true' calorimetric signal. This lag is primarily due to the delay in equilibration between the sample temperature and the program temperature when scan rates are too fast. A number of factors can contribute to the delay, including the masses of the sample, the reference material, and certain calorimeter components. For sample masses of the order of 100 mg, the lag time can be as much as 10 times the normal 5 s instrumental time constant [51], in agreement with the value of τ_{lag} (see Section 2.2.2). Examination of Fig. 3 shows that the data depart from linearity for scan rates >40°C min^{-1}. As a result, T_p values for high scan rates are greater than expected from an extrapolation of the data for low scan rates.

Isothermal data can be corrected for time lag effects either by methods described previously [31,32] or by eliminating data for which the precipitation time constant is small compared to τ_{lag}. Similarly, for DSC experiments we can define a scan rate which is 'too fast' by comparing τ_{lag} to the ratio of $\Delta T/S$, where ΔT is the temperature breadth of the precipitation peak. In order to minimize the effects of time lag, we suggest that scan rates should satisfy the following inequality:

$$\Delta T/(dT/dt) = \Delta T/S > \tau_{lag}. \quad (8)$$

This relation states that the time to scan through the peak width should be longer than the time lag [52]. For the data of Fig. 1, $\Delta T \approx 40$°C. As already mentioned, the lag time is of the order of 1 min. Thus, the Kissinger analysis of scans for ACO 339 should include only data for $S<40$°C min^{-1}. The solid curve in Fig. 3 was obtained by fitting Eq. (1) to data from experiments with scan rates ranging 1.2–20°C min^{-1}. The resulting activation energy is given in Table 3.

4.2. Isothermal calorimetry

4.2.1. 2-Exponential and rate-averaged time constants

As already pointed out, the 2-exponential equation describes individual isothermal dQ/dt plots better than does the Avrami expression, even though four adjustable parameters are required to fit each equation (α_1, α_2, τ_1 and τ_2 for the 2-exponential model; C, Δt, τ and n for the Avrami model). This result is consistent with the fact that two or more processes are contributing to precipitation in air-cooled alloy 339 [47], even though only a single peak is observed in scanning experiments.

In Section 4.2.2, we compare the DIC average time constants, τ_{rate} and τ_{Avrami}, to the effective average time constant from the Kissinger analysis.

4.2.2. Comparison of average time constants from DSC and DIC

Although more than one process seems to contribute to precipitation in air-cooled alloy 339, each scan of Fig. 1 exhibits only a single peak. Thus, rate constants, k, derived from the Kissinger analysis are average values, and effective average time constants are given by $1/k$. Fig. 8 compares the three average time constants, $1/k$, τ_{rate} and τ_{Avrami}, for air-cooled alloy 339. We see that $1/k$ and τ_{rate} agree very well, but they differ to a greater extent with τ_{Avrami}, suggesting that the latter is less suitable as an average measure of precipitation kinetics for ACO alloy 339. This conclusion is supported by the fact that the Avrami equation does not fit experimental dQ/dt curves as well as the 2-exponential model (Fig. 2). Thus, it appears that the DSC/Kissinger time constant $1/k$ is

Table 3
Precipitation activation energies (kJ/mol). Air-cooled aluminum alloy 339

Scanning calorimetry	Isothermal calorimetry			
Kissinger analysis	From τ_1	From τ_2	From τ_{rate}	From τ_{Avrami}
103.8±5.9	105.1±5.4	90.4±5.4	105.9±4.29	6.3±2.9

Note: Kissinger analysis result is from fit which excludes T_p values for scan rates of 40 and 80°C min^{-1}.

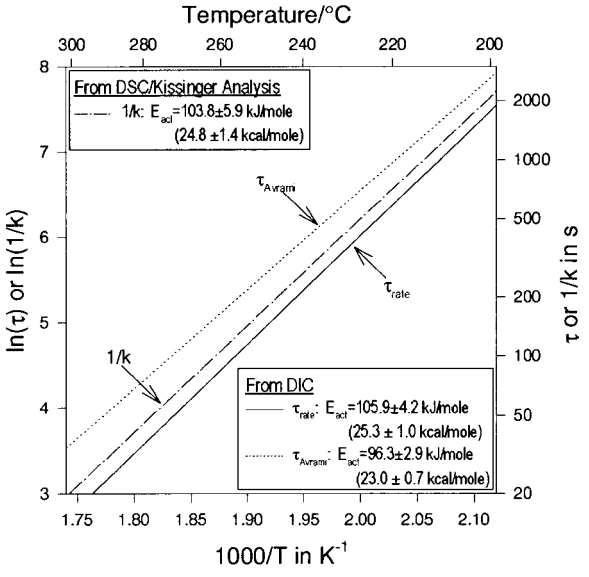

Fig. 8. Arrhenius plots of average time constant regression fits for air-cooled alloy 339. For DSC the average time constant is the reciprocal of the Kissinger rate constant ($1/k$); for DIC, two average time constants are shown (τ_{rate} and τ_{Avrami}). Agreement of $1/k$ and τ_{rate} is very good (see text).

essentially equivalent to the DIC time constant τ_{rate}, at least for air-cooled aluminum alloy 339.

5. Summary

Several significant findings resulted from the present work. These include aspects relevant to the measurement and analysis techniques as well as to the alloy studied.

5.1. Measurement and analysis techniques

The Kissinger analysis of scanning calorimetry data requires the temperature scan rate, S, to be slow compared to the instrumental lag time, τ_{lag}. If the inequality $\Delta T/S > \tau_{\text{lag}}$ is obeyed, the DSC/Kissinger method yields time constants and activation energies consistent with those from differential isothermal calorimetry, at least in the present example.

For isothermal experiments, in which two or more simultaneous precipitation processes are occurring, the rate-averaged time constant appears to be a more useful average τ than does the Avrami time constant.

5.2. Results for alloy 339

The activation energy from the Kissinger analysis (E_{act}=103.8 kJ/mol) agrees well with the value from an Arrhenius plot of rate-averaged isothermal time constants (E_{act}=105.9 kJ/mol). The value of E_{act} from τ_{Avrami} is somewhat lower (E_{act}=96.3 kJ/mol). A plot of the DSC/Kissinger average time constant, $1/k$, is nearly identical to that of the isothermal average, τ_{rate}, across the temperature range of the experiments (200–300°C). Agreement with τ_{Avrami} is not so good. However, as mentioned above, we have concluded that the Avrami time constant is perhaps less suitable as a measure of average precipitation kinetics.

We have shown that both *time constants* and *activation energies* for precipitation in air-cooled alloy 339, as determined by DSC and DIC, are in good agreement. However, additional studies are needed to further validate the equivalence of the techniques for calorimetrically more complex systems, such as solution-treated alloys which exhibit GP zone formation and dissolution, as well as precipitation [53].

Acknowledgements

The author thanks Anil Sachdev for supplying the samples and for several useful discussions; Coleman Jones for providing the casting; Raja Mishra for discussions of his TEM results; Dick Hall for machining samples to DSC size; Dan Hayden and Martin Meyer for assistance with computer-related problems; Tom Van Steenkiste for improvements to the calorimeters; and Dusanka Radovic for running several DSC7 scans. I also appreciate comments regarding the manuscript made by Bill Baxter and Anil Sachdev and a useful discussion with Bruce Cassell. The assistance of the General Motors Research and Development Library in obtaining several obscure references is also appreciated.

References

[1] J.M. Papazian, Met. Trans. 12A (1981) 269.
[2] J.M. Papazian, Met. Trans. 13A (1982) 761.
[3] M. Van Rooyan, J.A. Sinte Maartensdijk, E.J. Mittemeijer, Met. Trans. 19A (1988) 2433.

[4] C. Antonione, F. Marino, G. Riontino, Mat. Chem. and Phys. 20 (1988) 13.
[5] S. Abis, G. Donzelli, J. Mat. Sci. Letters 7 (1988) 51.
[6] J.M. Papazian, Met. Trans. 19A (1988) 2945.
[7] A.K. Jena, A.K. Gupta, M.C. Chaturvedi, Acta. Metall. 37 (1989) 885.
[8] M.C. Chaturvedi, A.K. Gupta, A.K. Jena, Mat. Sci. and Eng. A110 (1989) 187.
[9] M. Van Rooyen, E.J. Mittemeijer, Met. Trans. 20A (1989) 1207.
[10] I. Dutta, D.L. Bourell, Mat. Sci. and Eng. A112 (1989) 67.
[11] C. Badini, F. Marino, A. Tomasi, Mater. Chem. and Phys. 25 (1990) 57.
[12] A.-M. Zahra, C.Y. Zahra, J. Thermal Anal. 36 (1990) 1465.
[13] C. Badini, F. Marino, A. Tomasi, Mater. Sci. and Eng. A136 (1991) 99.
[14] M.J. Starink, P. Van Mourik, Met. Trans. 20A (1991) 665; M.J. Starink, V. Jooris, P. van Mourink, in: N. Hansen et al. (Eds.), Metal Matrix Composites – Processing, Microstructure and Properties, Risϕ National Lab, Roskilde, Denmark, 1991, p. 675.
[15] H.-L. Lee, W.-H. Lu, S.L.-I. Chan, Scripta Met. et Mat. 25 (1991) 2165.
[16] I. Dutta, S.M. Allen, J.L. Hafley, Met. Trans. 22A (1991) 2553.
[17] M.J. Starink, P. van Mourik, Mat. Sci. and Eng. A156 (1992) 183; M.J. Starink, A.M. Zahra, Thermochimica Acta 292 (1997) 159.
[18] T.S. Kim, T.H. Kim, K.H. Oh, H.I. Lee, J. Mater. Sci. 27 (1992) 2599.
[19] I. Dutta, C.P. Harper, G. Dutta, Metallurg. and Materials Trans. 25A (1994) 1591.
[20] C. Garcia-Cordovilla, E. Louis, J. Narciso, A. Pamies, Mat. Sci. and Eng. A189 (1994) 219.
[21] M.P. Thomas, J.E. King, J. Mat. Sci. 29 (1994) 5272.
[22] C. Badini, F. Marino, E. Verne, Mat. Sci. and Eng. A191 (1995) 185.
[23] I.N.A. Oguocha, S. Yannacoupoulos, Mat. Sci. and Eng. A231 (1997) 25.
[24] H.E. Kissinger, Anal. Chem. 29 (1957) 1702.
[25] T. Ozawa, J. Thermal Anal. 2 (1970) 301.
[26] R.L. Thakur, in: Advances in Nucleation and Crystallization of Glasses, Am. Ceram. Co., Columbus, 1972, p. 166 (cited in Ref. [29]).
[27] J.A. Augis, J.E. Bennett, J. Therm. Anal. 13 (1978) 283.
[28] E.J. Mittemeijer, L. Cheng, P.J. van der Schaaf, C.M. Brakman, B.M. Korevaar, Met. Trans. 19A (1988) 925.
[29] H. Yinnon, D.R. Uhlmann, J. Non-Crystalline Solids 54 (1983) 253.
[30] J. Sestak, in: G. Svehla (Ed.), Comprehensive Analytical Chemistry, vol. XII, Part D, Elsevier, Amsterdam, 1984, p. 212, Ch. 9.
[31] G.W. Smith, Scripta Met. et Mat. 31 (1994) 357.
[32] G.W. Smith, Thermochimica Acta 291 (1997) 59.
[33] G.W. Smith, Thermochimica Acta 112 (1987) 289, (Refs. [33-38] illustrate application of DIC to phase separation and cure kinetics in liquid crystal/polymer systems).
[34] G.W. Smith, N.A. Vaz, Liq. Cryst. 3 (1988) 543.
[35] G.W. Smith, Mol. Cryst. Liq. Cryst. 180B (1988) 201.
[36] G.W. Smith, Mol. Cryst. Liq. Cryst. 196 (1991) 89.
[37] G.W. Smith, Int. J. Modern Phys. B7 (1993) 4187.
[38] G.W. Smith, Mol. Cryst. Liq. Cryst. 239 (1994) 63.
[39] A. Zahra, in: H. Brodowsky, H.-J. Schaller (Eds.), Thermochemistry of Alloys, Kluwer Acad. Pub., 1989, p. 203.
[40] A. Zahra, C.Y. Zahra, M. Laffitte, Z. Metallkunde 70 (1970) 669.
[41] A. Zahra, C.Y. Zahra, M. Laffitte, W. Lacom, H.P. Degischer, Z. Metallkunde 70 (1979) 172.
[42] W. Lacom, H.P. Degischer, A. Zahra, C.Y. Zahra, High Temperatures – High Pressures 12 (1980) 549.
[43] A. Zahra, C.Y. Zahra, J.C. Mathieu, Z. Metallkunde 71 (1980) 54.
[44] A. Zahra, C.Y. Zahra, J. Dutkiewicz, R. Ciach, J. Mat. Sci. 25 (1990) 391.
[45] W. Lacom, C.Y. Zahra, A.M. Zahra, Scripta Met. 23 (1989) 2001.
[46] M.J. Starink, A.M. Zahra, Materials Sci. Forum 217–222 (1996) 795.
[47] In TEM studies of aluminum alloy 339, R.K. Mishra (private communication) observed three or four precipitate phases, including Q ($Al_5Cu_2Mg_7Si_7$), θ' (Cu_2Al), and β' (Mg_2Si). This work will be published elsewhere. His results are consistent with those of Starink et al. [14], Dutta et al. [19]. The former detected Q and θ' precipitates in Al/3.5Cu/1.0Mg/20Si; the latter found λ' ($Al_5Cu_2Mg_8Si_5$) and θ' phases in Al/4.6Cu/0.4Mg/0.7Si.
[48] In a chemical reaction consisting of several simultaneous elementary steps the overall reaction rate is given by adding the rates of the steps. (See, for example, G.W. Castellan, Physical Chemistry, Addison-Wesley, Reading, MA, 1964, p. 614).
[49] For ACO alloy 339, τ_{lag} is small, so that relatively few data points are excluded from fits of Eq. (7).
[50] Jandel Scientific, San Rafael, CA.
[51] Bruce Cassell, private communication.
[52] Constraints on the heating rate have also been discussed in Ref. [3]. These workers use scan rates of 5 to 40°C min^{-1}. Since their precipitation peaks are somewhat broader than in the present case, their use of the higher scan rate seems consistent with expression (8) of the present work.
[53] Such studies have indeed been completed for a solutionized aluminum alloy, and a paper has been submitted for publication.